Table IV. Activation Parameters for the Iron(II) Reduction of Some Bromo- and Chlorocobalt(III) Complexes

Complex	$\Delta H^{\ddagger}$, kcal/mol	$\Delta S^{\ddagger}$, eu	$\Delta G^{\ddagger}$, kcal/mol	Ref
cis-$[Co(eee)Br_2]^+$	12.1	−22.9	18.9	This work
cis-$[Co(eee)Cl_2]^+$	10.5	−22.6	17.2	This work
$[Co(NH_3)_5Br]^{2+}$	15.5	−20.14	21.6	11
$[Co(NH_3)_5Cl]^{2+}$	12.5	−30	21.5	14
cis-$[Co(en)_2(NH_3)Br]^{2+}$	17.6	−23.2	24.5	11
cis-$[Co(en)_2(OH_2)Br]^{2+}$	15.4	−23.2	22.3	11

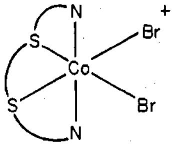

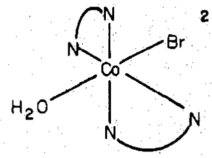

pertinent axis is fairly weak. Also H_2O can diffuse with solvent assistance into the bulk solvent quite readily. These factors lower the e_g acceptor orbital on Co(III) and a rapid reduction of *trans*-$Co(en)_2H_2OBr^{2+}$ is observed. In the case of *s-cis*-$Co(eee)Br_2^+$, the axis at which reaction occurs is also influenced by a weaker average crystal field strength due to Br^- and R–S–R donor. The problem arises in our ability to envision the movement of the R–S–R donors away from the Co(III) center and into the bulk solvent, prior to electron transfer. Molecular models and stereochemical studies[9,10] strongly suggest that the chelate ring conformations are quite rigid and that appreciable mobility of the R–S–R donor is lacking. Furthermore, the effect of increased chelation tends to slow down reduction processes between Fe(II) and Co(III) complexes.[12]

We believe the reason for the marked increase in the rate coefficient for the reduction of *s-cis*-$Co(eee)Br_2^+$ is due to the presence and interaction of the thioether donor atoms in the ligand eee. A similar significant rate increase has previously been observed for the corresponding dichloro-[2] and oxalatocobalt(III)[3] complexes containing eee. The explanation we advance for this observation is that the empty low-lying d orbitals of sulfur interact with the Co(III) molecular orbitals promoting significant M→L back-bonding within the complex. This Co(III)–S association lowers the oxidant's acceptor orbital energy, facilitating transfer of an electron from the Fe(II) reductant to the oxidant. Experimentally one observes an enhanced overall rate of reduction for the eee series of compounds as compared to ammine and ethylenediamine complexes.

This concept is further strengthened by the recent work of Rorabacher and co-workers,[8] who demonstrate that thiaether-containing ligands stablize the lower oxidation state in complexes of the type $Cu^{I}eee^+$ as opposed to $Cu^{II}eee^{2+}$. In contrast, the presence of NH_2 and/or HN< donors within a linear tetradentate ligand design creates the opposite effect, stabilizing the metal in a higher oxidation state and destabilizing the lower oxidation state.

Bifano and Linck[17] suggest that the parameter most likely to influence the energy of the acceptor orbital in Fe(II)–Co(III) systems is the σ component of the bonding strength for the nonbridging ligands. The smaller the σ contribution, the more rapid the observed reduction rate. The σ component concept can be invoked as a possible explanation in the eee series; however, is it in reality substantially different from Orgel's original crystal field strength (CFS) suggestions? Are not CFS and σ donor strength one in the same when applied to the above problem?

It is interesting to note that the point one obtains by plotting $\log k_{Br^-}$ vs. $\log k_{Cl^-}$ for *s-cis*-$Co(eee)Br_2^+$ and *s-cis*-$Co(eee)Cl_2^+$ does not fall within the proximity of the line Linck obtained for a series of ammine and ethylenediamine bromo- and chlorocobalt(III) complexes reacting with Fe(II).[11] The established reactivity pattern, $k_{Cl^-} > k_{Br^-}$, however, is mantained in the eee series.

The high reactivity of *s-cis*-$Co(eee)Br_2^+$ and *s-cis*-$Co(eee)Cl_2^+$ when compared with the traditional amine and ethylenediamine complexes is caused primarily by the change in $\Delta H^{\ddagger}$. Table IV presents the activation parameters for a series of related complexes. The data are consistent with the observations and conclusions of Linck[11] and the quantitative analysis of Hush[18] that in this comparison the enthalpy of activation reflects a perturbution of the Co(III) center by the nonbridging ligands and is primarily electronic in nature, reducing the energy of the acceptor orbital of the oxidant.

Reports concerning the kinetic and electronic influences exerted by coordinated sulfur are quite limited. Future work in this laboratory is designed to examine more closely the electronic role of coordinated sulfur ligands.

Registry No. *s-cis*-$Co(eee)Br_2^+$, 46135-49-3; *s-cis*-$Co(eee)Cl_2^+$, 32594-33-5; Fe^{2+}, 15438-31-0.

References and Notes

(1) L. E. Bennett, *Prog. Inorg. Chem.*, **18**, 1 (1973).
(2) J. H. Worrell and T. A. Jackman, *J. Am. Chem. Soc.*, **93**, 1044 (1971).
(3) J. H. Worrell, R. A. Goddard, E. M. Gupton, Jr., and T. A. Jackman. *Inorg. Chem.*, **11**, 2734 (1972).
(4) C. J. Weschler and E. Deutsch, *Inorg. Chem.*, **15**, 139 (1976).
(5) J. M. Palmer and E. Deutsch, *Inorg. Chem.*, **14**, 17 (1975).
(6) L. E. Asher and E. Deutsch, *Inorg. Chem.*, **15**, 1531 (1976).
(7) T. A. Jackman, Ph.D. Thesis, University of South Florida, 1976.
(8) E. R. Dockal, T. E. Jones, W. F. Sokol, R. J. Engerer, D. B. Rorabacher, and L. A. Ochrymowycz, *J. Am. Chem. Soc.*, **98**, 4322 (1976).
(9) J. H. Worrell and D. H. Busch, *Inorg. Chem.*, **8**, 1563 (1969).
(10) B. Bosnich, W. R. Kneen, and A. T. Phillip, *Inorg. Chem.*, **8**, 2567 (1969).
(11) R. G. Linck, *Inorg. Chem.*, **9**, 2529 (1970).
(12) P. Benson and A. Haim, *J. Am. Chem. Soc.*, **87**, 3826 (1965).
(13) A. Haim and N. Sutin, *J. Am. Chem. Soc.*, **88**, 5343 (1966).
(14) J. H. Espenson, *Inorg. Chem.*, **4**, 121 (1965).
(15) R. G. Linck, *Surv. Prog. Chem.*, **7**, 89 (1976).
(16) J. E. Earley, *Prog. Inorg. Chem.*, **13**, 243 (1970).
(17) C. Bifano and R. G. Linck, *J. Am. Chem. Soc.*, **89**, 3945 (1967).
(18) N. S. Hush, *Prog. Inorg. Chem.*, **8**, 391 (1967).

Contribution from Philips GmbH Forschungslaboratorium
Aachen, D 5100 Aachen, Federal Republic of Germany,
and Max-Planck-Institut für Festkörperforschung,
D 7000 Stuttgart 80, Federal Republic of Germany

Occurrence of Corundum-Type Indium(III) Oxide under Ambient Conditions

G. Frank,* R. Olazcuaga,[1] and A. Rabenau

Received November 23, 1976 AIC608542

At room temperature and ambient pressure, the Mn_2O_3-type modification (space group *Ia*3) is the stable form of In_2O_3 (In_2O_3(I)). The unit cell is derived from a distorted fluorite structure with one-fourth of the anion sites being unoccupied.[2]

The existence of a high-temperature, high-pressure rhombohedral modification of In_2O_3 (In_2O_3(II)) with the corundum structure (space group $R\bar{3}c$) has been reported in the literature.[3-5] This phase is 2.5% denser than cubic In_2O_3(I); the cation–anion distances are nearly the same but the anion packing is somewhat distorted from a close-packed hexagonal arrangement without vacancies, the distortion, however, being smaller than that of In_2O_3(I).[5] Shannon obtained small crystals of In_2O_3(II) at 1250 °C and 65 kbars,[3] and Christensen et al.[4] observed the occurrence of In_2O_3(II)

---

* To whom correspondence should be addressed at Philips GmbH Forschungslaboratorium Aachen.

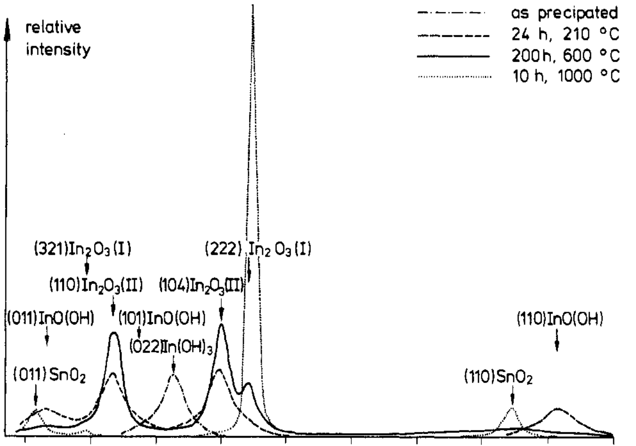

Figure 1. X-ray diffractograms of In_2O_3–SnO_2 coprecipitate containing 15 atom % tin, after annealing at different temperatures.

crystals in the In_2O_3–$H_2O(D_2O)$–Na_2O system around 350–400 °C and 150–400 bars; they considered In_2O_3(II) as a metastable phase under these conditions. Later, Prewitt et al.[5] reported, besides other high-pressure experiments, the growth of 0.5-mm diameter In_2O_3(II) crystals, in NaOH as a flux, at 1000 °C and 44 kbars.

Experimental Section

In contrast to the high-pressure conditions mentioned above, we obtained In_2O_3(II) with some dissolved SnO_2 at ambient pressure. Extensive tests showed that the following experimental conditions should be observed. Two-tenths molar solutions of $InCl_3$ (Merck, LAB) and $SnCl_4$ (Merck, p.a.) were mixed in various proportions, heated to 50–90 °C, and stirred (100–200 rpm). Indium hydroxide and stannic acid were coprecipitated by neutralizing the solution with NH_4OH (1 part of NH_4OH (25%); 1 part of H_2O) to pH 7. About 30 mL of cold saturated NH_4NO_3 solution was added per gram of precipitate after the precipitation to promote the coagulation of the gels. The precipitate was filtered, washed with NH_4NO_3 solution until the filtrate was free of Cl^- ions, dried at 200–220 °C during 15 h, and transformed into the oxides by annealing in Al_2O_3 crucibles at 500–600 °C in air for about 10 h. The total yield was about 95–99%.

Results and Discussion

The powders were analyzed by x-ray diffractometry. The as-precipitated gels consisted mainly of $In(OH)_3$;[4] they were transformed into InO(OH)[6] by heating at about 200 °C. Depending on the composition of the starting solution and the precipitation temperature, the lines of In_2O_3(I), In_2O_3(II), and SnO_2 were observed after annealing at about 600 °C (Figure 1). The x-ray reflections of the two In_2O_3 phases were relatively sharp, while those of SnO_2 were diffuse, indicating a particle diameter of $\gtrsim$100 nm for In_2O_3 and of about 10 nm for SnO_2.[7] The relative intensities of the x-ray reflections of In_2O_3(II) agreed with those given in the literature.[5] The In_2O_3(II) could be completely transformed into In_2O_3(I), if the powder mixtures were annealed in air at temperatures $\gtrsim$900 °C for some hours. The SnO_2 particles coarsened during this process (Figure 1).

Recently, Varfolomeev et al.[8] reported similar results of In_2O_3–SnO_2 mixtures, based on coprecipitates obtained from solutions of the respective nitrates. Their published *d* values and intensities, which they provisionally ascribed to a compound In_2SnO_5, are in complete agreement with the data given by Prewitt et al.[5] for In_2O_3(II).

On taking the areas of the most intensive x-ray reflections as a measure of the concentrations of the respective phases and on comparison of the results of the coprecipitates with those of In_2O_3–SnO_2 mixtures prepared from separate oxides, about 5–8 atom % of tin appears to be dissolved in In_2O_3, irrespective of whether In_2O_3(II) is present or not.

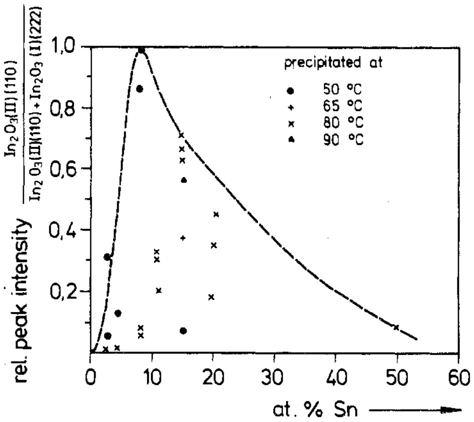

Figure 2. Relative yield of In_2O_3(II). Parameters are tin concentration and precipitation temperature. All samples were annealed at 550 °C, 24 h.

The relative amount of In_2O_3(II) depends on the preparation conditions. From the experimental results available, the following conclusions can be drawn.

(a) The addition of tin ions to the $InCl_3$ solution is essential in order to obtain In_2O_3(II).

(b) Addition of $SnCl_4$ results in considerably more In_2O_3(II) than addition of $SnCl_2 \cdot 2H_2O$. Mössbauer spectra showed the presence of only Sn^{4+} in the oxides in both cases.

(c) A maximum yield of In_2O_3(II) is obtained, if the tin concentration corresponds to about 5–8 atom %, the precipitation temperature is about 50 °C, and the annealing temperature is about 500 °C. Roentgenographic single-phase In_2O_3(II) has been obtained under these conditions (Figure 2).

(d) NO_3 ions, preferentially from NH_4NO_3, promote the formation of In_2O_3(II). The NH_4NO_3 solution is preferably added to the hot precipitate immediately after the precipitation. (No In_2O_3(II) could be detected if NH_4Cl was added instead of a nitrate.)

The following model for the formation of In_2O_3(II) under ambient conditions is tentatively proposed. In the series of M_2O_3 oxides (M = metal), those having small cations with effective ionic radii $\lesssim$0.07 nm form stable corundum-type phases under ambient conditions.[5] The ionic radius of In^{3+} is 0.081 nm. The replacement of In^{3+} by the smaller (r = 0.071 nm) Sn^{4+}, accompanied by the formation of cation vacancies for charge compensation, corresponds to a reduction of the effective cation radius and therefore points in the direction of a stabilization of the corundum structure. In agreement with this model, the maximum yield of this (still metastable) corundum-type In_2O_3(II) is obtained if the concentration of Sn^{4+} corresponds to the solubility limit of 5–8 atom % tin in In_2O_3.

The role of NO_3^- is still an open question. From the fact that the NO_3^- ions are added after the precipitation is completed, one may conclude that they play a part during the transformation of the gels into the oxides. Maybe they are adsorbed at the gel molecules and thereby influence the nucleation process of the oxides.

Acknowledgment. The authors are grateful to Mrs. L. Brock for part of the preparations and to Mr. H. D. Bausen for the x-ray measurements.

Registry No. In_2O_3(II), 1312-43-2.

References and Notes

(1) On leave from the Laboratoire de Chimie du Solide du CNRS, 33405 Talence, France.
(2) W. H. Zachariasen, *Nor. Geol. Tidsskr.*, **9**, 310 (1927); M. Marezio, *Acta Crystallogr.*, **20**, 723 (1966).

(3) R. D. Shannon, *Solid State Commun.*, **4**, 629 (1966).
(4) A. N. Christensen, N. C. Broch, O. v. Heidenstam, and A. Nilsson, *Acta Chem. Scand.*, **21**, 1046 (1967).
(5) C. T. Prewitt, R. D. Shannon, D. B. Rogers, and A. W. Sleight, *Inorg. Chem.*, **8**, 1985 (1969).
(6) A. N. Christensen, R. Gronbaek, and S. E. Rasmussen, *Acta Chem. Scand.*, **18**, 1261 (1964).
(7) B. D. Cullity, "Elements of X-Ray Diffraction", Addison-Wesley, Reading, Mass.
(8) M. B. Varfolomeev, A. S. Mironova, F. Kh. Chibirova, and V. E. Plyushchev, *Inorg. Mater.* (*Engl. Transl.*), **11**, 1926 (1975); *Izv. Akad. Nauk SSSR, Neorg. Mater.*, **11**, 2242 (1975).
(9) The tin concentrations of the precipitates were checked by x-ray fluorescence analysis after annealing.

Contribution from the Department of Chemistry,
Indiana University, Bloomington, Indiana 47401

Organogold(III) Complexes. Structure of Monomethyldibromogold

S. Komiya, J. C. Huffman, and J. K. Kochi*

Received December 13, 1976 AIC608901

Organogold complexes[1] are valuable probes for the study of reductive elimination of organometallic intermediates in catalytic reactions.[2] Thus, trimethyl- and dimethyl(anionо)gold complexes with the formulations $(CH_3)_3AuL$ and $(CH_3)_2XAuL$, respectively [L = phosphines], afford only the homonuclear CH_3–CH_3 on reductive elimination.[1,3] We sought to examine the heteronuclear elimination of CH_3–X from the corresponding monomethyl analogues, $CH_3(X)_2AuL$. However, despite a number of efforts to synthesize such monoalkylgold(III) complexes, there are no unambiguous examples extant,[4] and it is generally concluded that they are unstable.[6,7] Attempts to prepare monoalkyldibromogold by electrophilic brominolysis of the dimeric dialkylbromogold according to eq 1 indeed led to compound I [R = ethyl, *n*-propyl] with the correct empirical formula.[6] Although it was recognized that two structures, the symmetric II (trans and cis) as well as the unsymmetric III, were possible, they could not be distinguished on the basis of chemical studies and dipole measurements.[6] Since these efforts represent a potentially valuable route to the desired monoalkylgold(III) complexes, we examined the structure of the methyl analogue of I in detail.

$$[R_2AuBr]_2 + 2Br_2 \rightarrow \underset{\text{I}}{[RAuBr_2]_2} + 2RBr \qquad (1)$$

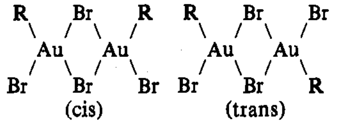
(cis) (trans)

II

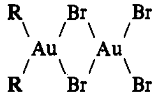
III

Experimental Section

Materials. The gold complexes, $[(CH_3)_2AuBr]_2$, $(CH_3)_2XAuPPh_3$ [X = Br, I], $BrAuPPh_3$, CH_3AuPPh_3, were prepared using published procedures.[3,8] The halogenophospines, $X^-XPPh_3^+$ [X = Br, I], were synthesized from X_2 and PPh_3.[9] A colorless solution of $[(CH_3)_2AuBr]_2$ (25.0 mg) in CCl_4 (1.0 ml) was treated with bromine (5.5 μL) to give a red solution which gradually deepened and then lightened on standing for 3 days at room temperature as dark red crystals of IV separated from solution. During this change the singlet (δ 1.40) in the ^1H NMR spectrum of $[(CH_3)_2AuBr]_2$ decreased concomitantly with an increase in that due to CH_3Br (δ 2.55) which was finally formed in 75% yield. The solution on further standing at room temperature gradually evolved ethane. Compound IV forms transparent dark red crystals when freshly prepared, but gradually changes in solution or in the solid state to an opaque black solid within a week. All ^1H NMR spectra were recorded on a Varian EM360 spectrometer using external TMS standards.

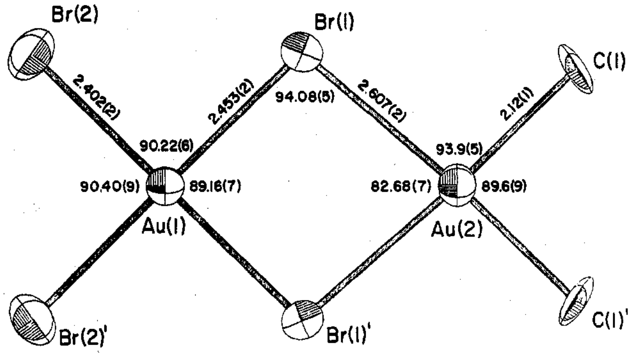

Figure 1. ORTEP drawing of the molecule showing bonded distances and angles. Primed atoms are related to nonprimed atoms by a twofold axis which passes through the two gold atoms. Thermal ellipsoids are drawn at the 50% probability level. The gold–gold distance is 3.705 (1) Å, where the number in parentheses represents the error in the least significant digits.

X-Ray Crystallographic Study of IV. A crystal of dimensions 0.70 × 0.078 × 0.064 mm was placed in a gaseous nitrogen cold stream on the goniostat and maintained at −160 ± 5 °C throughout characterization and data collection. The diffractometer used consisted of a Picker four-circle goniostat with a graphite monochromator (002 plane), and a Texas Instruments T1980B minicomputer. The goniostat was controlled by stepping motors using locally designed interfaces and programs.

The crystal was characterized on the goniostat and found to be $C2/c$ with $a = 12.202$ (2) Å, $b = 10.722$ (2) Å, $c = 7.673$ (2) Å, and $\beta = 94.19$ (1)° at −160 °C as determined by a least-squares fit of angular data from 12 centered reflections. The calculated density for $Z = 4$ is 4.93 g/cm^3. Redundant intensity data were collected by 2θ scan techniques (4°/min) to a maximum of $2\theta = 55°$. The intensity data were reduced in the usual manner,[10] corrected for Lorentz–polarization terms and absorption (μ 449.3 for λ(Mo Kα) 0.71069 Å), and reduced to the 1152 unique structure amplitudes. The 1125 structure amplitudes with $F_o^2 > \sigma(F_o^2)$ were considered "observed" and used in all calculations. An ignorance factor of 0.06 was used in the data reduction formula.

The structure, which possesses crystallographic twofold symmetry, was solved by a combination of direct and Patterson techniques and refined anisotropically by full-matrix least-squares.[11] The function minimized was $\sum w(|F_o| - |F_c|)^2$ in which w is $4F_o^2/\sigma^2(F_o^2)$. The final residuals were $R(F) = 0.058$ and $R_w(F) = 0.050$, where $R(F)$ and $R_w(F)$ are defined as $\sum||F_o| - |F_c||/\sum|F_o|$ and $[\sum w(|F_o| - |F_c|)^2/\sum wF_o^2]^{1/2}$. The "goodness of fit" for the last cycle was 1.68, and the largest Δ/σ was 0.03. A final difference Fourier synthesis was featureless except for peaks of 2.2 and 2.1 e/Å^3 remaining in the location of the gold atoms.

Results and Discussion

Treatment of dimethylbromogold with an equimolar amount of bromine in carbon tetrachloride solution at room temperature afforded high yields of methyl bromide, and methyldibromogold (IV) separated from solution as dark red crystals according to eq 2.

$$[(CH_3)_2BrAu]_2 + 2Br_2 \rightarrow \underset{\text{IV}}{2CH_3(Br_2)Au} + 2CH_3Br \qquad (2)$$

To avoid decomposition, the diffraction data were collected on a freshly prepared transparent crystal of IV held at −160 °C. The molecular structure of IV in Figure 1 is planar and consists of discrete dimeric units of two gold atoms, each in a square-planar configuration and held with two bridging bromine atoms. Importantly, both methyl groups in the dimer are bonded to the same gold atom. The bond distances and bond angles in Figure 1 and Table I are comparable to those found in the binuclear structure in $[(CH_3CH_2)_2AuBr]_2$.[12]